Systematic study of heavy-cluster radioactivity from superheavy nuclei

O. N. Ghodsi,* M. Morshedloo, and M. M. Amiri†
Department of Physics, Faculty of Science, University of Mazandaran, P.O. Box 47415-416, Babolsar, Iran

(Received 4 December 2023; accepted 11 January 2024; published 15 February 2024)

This study investigates the probable heavy-cluster radioactivity from superheavy nuclei with $100 \leqslant Z \leqslant 120$ using the modified double-folding formalism by applying the Pauli exclusion principle. To this aim, the half-lives of the most probable cluster radioactivity are investigated by applying the Pauli exclusion principle to the internal energy of the dinuclear system. The results indicated that considering Pauli blocking as a modification term in calculating the double-folding potential leads to more consistent half-lives with the predictions of other theoretical models. Also, the competition between α decay and heavy-cluster radioactivity at the superheavy region is investigated. The obtained results show that the cluster radioactivity can be expected for some superheavy nuclei with $Z = 120$.

DOI: 10.1103/PhysRevC.109.024612

I. INTRODUCTION

Experimental and theoretical studies on the superheavy nuclei (SHN) have become one of the active current areas in nuclear physics. To date, the elements with atomic number Z up to 118 have been synthesized by cold- and hot-fusion reactions through neutron-evaporation channels [1–9]. It is well known that analyses of the decay modes of SHN are a very important tool for understanding the nuclear structure, and the information about new isotopes due to the newly formed isotopes is confirmed by observing their decay properties. Hence, accurate predictions for the heavy-cluster-decay half-lives of SHN would be required to synthesize new elements.

On the other hand, the α decay is recognized as one of the most important decay modes of the unstable SHN, which can be considered as a probe for identifying synthesized SHN in the laboratory [10–12]. Investigations of α decay can provide reliable knowledge on the structure and properties of SHN, such as half-lives, radius, shell effect, nuclear spins and parities, and deformation [13–18]. Thus, many phenomenological and microscopic models have been adopted to investigate the properties of the α-decay processes from SHN based on the quantum tunneling effect of Gamow [19–28].

In addition, cluster radioactivities would also be a probable phenomenon in the superheavy region, observed experimentally [29–31]. The cluster radioactivity was first suggested by Sandulescu *et al.* theoretically [32], and then the experimental evidence of the prediction was observed by Rose and Jones [33]. Later, it was confirmed by Aleksandrov *et al.* that the ^{14}C cluster was found to be emitted from ^{223}Ra [34]. From then on, many kinds of clusters, such as ^{18,20}O, ^{23}F, $^{22,24-26}$Ne, ^{28,30}Mg, and ^{32,34}Si, were observed experimentally from heavy nuclei ranging from $Z = 87$ to $Z = 96$ [35–42]. Extensive theoretical methods have been proposed to successfully describe cluster radioactivity from heavy nuclei [40–42]. These models can be classified by the α-like or fissionlike theories [40].

Very recently, Poenaru *et al.* extended the concept of cluster radioactivity to heavy-cluster radioactivities to allow the emission of heavy particle ones up to $Z_{\max} = Z - 82$ from actinides and SHN with $Z > 110$ and daughters around ^{208}Pb [40,43,44]. The results claimed that some SHN with $Z = 104-124$ express shorter half-lives and larger clustering branching ratios than α decay. Moreover, many researchers have carried out analyses of the heavy-cluster radioactivities to investigate the possibility of heavy-cluster emission from SHN through various theoretical models [28,43,44]. For instance, the simultaneous studies of the α and cluster radioactivity of SHN with $Z = 104-124$ using an analytical super asymmetric fission model (ASAF) succeeded in estimating their dominant decay modes [43,44]. Also, the possibilities of heavy-cluster emissions from SHN using different universal formulas such as the unified description (UD) formula [45], the universal curve [46], the Horoi formula [47], and the universal decay law (UDL) [48] has been studied to estimate the half-lives of α decay and heavy-cluster radioactivities [28]. Furthermore, the α-decay and heavy-cluster-decay probabilities of superheavy isotopes have been studied using the Coulomb and proximity potential model (CPPM) to predict dominant decay modes for isotopes of $Z = 100-120$ [49]. Also, the simultaneous studies of the half-lives of α decay and heavy-cluster radioactivity of SHN based on the modified generalized liquid-drop model and the effective liquid-drop model evaluate the possibility of heavy-cluster emission from superheavy regions [50–54].

Considering the above investigations, the microscopic density-dependent cluster model based on preformed cluster formalism is also commonly used for describing α and cluster radioactivity [55–58]. In the framework of cluster radioactivity, formation probability is attributed to the cluster before the

*o.nghodsi@umz.ac.ir
†morteza.moghaddari@stu.umz.ac.ir

tunneling process in the Coulomb barrier of the parent nucleus [59–65]. Hence, each clusterization state would remarkably affect the products of decay processes and nucleon-nucleon (NN) interactions.

In addition, the nucleus-nucleus interaction potential plays a substantial role in describing the cluster-decay processes. Meanwhile, the overlapping densities of the participating nuclei could affect the interaction potential, which could be more apparent in the partial overlap region and the full overlap region [66–71]. Besides, the well-known density-dependent double-folding (DF) model with realistic M3Y effective NN interactions has been extensively used for describing the scattering data, fusion, and α-decay processes [72,73]. One should consider that the interaction potentials calculated by the DF model can well describe the tail region of the NN interaction potential but fail to describe many reactions strongly affected by the characteristics of the potential in the internal region [74].

This deficiency can be due to the nonconsideration of the repulsive core in the DF formalism [72]. However, the satisfactory and antisymmetrization impact of the Pauli exclusion principle (PEP) would substantially compensate for such insufficiencies [75]. Since the effect of Pauli blocking behaves as a repulsive force in the dinuclear system [76], such compensation would be manifested as increasing the intrinsic kinetic energy of the nuclear densities at small separation distances [77,78]. Hence, determining the kinetic energy and its association with the DF model could provide some dynamic aspects leading to more realistic results.

Employing the more realistic nucleon density distributions calculated by the self-consistent Hartree-Fock (HF) formalism, calculations of the heavy-cluster-decay half-lives within the association of the PEP with the DF formalism are carried out. The obtained results are also compared with the available data. Furthermore, the competition between α decay and the heavy-cluster radioactivity at the superheavy region is investigated by analyzing half-life branching ratios of heavy-cluster radioactivities and α clusters.

This paper is organized as follows. The formalisms of potential and half-life calculations are given in Sec. II, and our results and discussion are given in Sec. III. The main results and conclusions are provided in Sec. IV.

II. THEORETICAL FRAMEWORK

A. Double-folding formalism and the cluster-decay half-life

The total interaction potential between cluster and daughter nuclei plays a vital role in interpreting the heavy-cluster-decay process. The effective cluster-core potential $V_{\rm Tot}(R)$ is given by

$$V_{\rm Tot}(R) = V_N(R) + V_C(R) + \frac{\hbar^2}{2\mu}\frac{(\ell+1/2)^2}{R^2}, \qquad (1)$$

where $V_N(R)$, and $V_C(R)$ are the short-range attractive nuclear potential and the long-range Coulomb repulsive potential, respectively [61,79,80]. Also, R refers to the vector joining the center of masses of the two nuclei and μ denotes the reduced mass of the cluster-daughter nucleus system. Moreover, ℓ represents the orbital angular momentum carried away by the emitted cluster. The modification $\ell(\ell+1) \to (\ell+1/2)^2$ in the latter term of Eq. (1) represents the Langer modified centrifugal potential [79,81] that is essential for the first order validity of the Wentzel-Kramers-Brillouin (WKB) integral and the correct behavior of the scattering radial wave function near the origin [82,83].

In the framework of the DF model, the nuclear potential with effective NN interaction and the Coulomb potential can be obtained as [72,84]

$$V_{N(C)}(R) = \iint \rho_1(\mathbf{r}_1)\, v_{N(C)}(\mathbf{s})\rho_2(\mathbf{r}_2)\, d^3\mathbf{r}_1 d^3\mathbf{r}_2, \qquad (2)$$

where $\mathbf{s} = \mathbf{R} + \mathbf{r_1} - \mathbf{r_2}$ refers to the relative distance between one nucleon from the emitted cluster and the other nucleon in the daughter nucleus. Here, $\mathbf{r_1}$ and $\mathbf{r_2}$ are the vectors describing the positions of the nucleons belonging to the emitted cluster and the daughter nucleus relative to their centers of mass, respectively, and $v_{N(C)}(\mathbf{s})$ is the effective NN interaction or the standard proton-proton Coulomb force. Also, $\rho(\mathbf{r_1})$ and $\rho(\mathbf{r_2})$ are the density distribution of the spherical cluster and the daughter nuclei, respectively. In this study, such densities are determined by HF calculations based on the parametrization of Skyrme interactions [85] due to their capabilities for well reproducing the root-mean-square (rms) and cluster-decay energy of SHN.

Moreover, to calculate the nuclear potential, the M3Y-Reid-type interaction with zero-range exchange contribution is adopted and introduced as [84]

$$V_{\rm eff}(\mathbf{s}) = 7999\frac{\exp(-4s)}{4s} - 2134\frac{\exp(-2.5s)}{2.5s} + J_{00}\delta(\mathbf{s}),$$
$$J_{00} = -276(1 - 0.005E/A), \qquad (3)$$

where $E = A_2Q/(A_2+A_1)$ is the energy in the center-of-mass frame. Here, A_1 and A_2 represent the mass number of the emitted cluster and the daughter nuclei, respectively, and Q is the cluster-decay energy.

B. Cluster-decay half-lives

In the present study, the half-life of the parent nucleus against the split into a heavy cluster and a daughter nucleus is $T_{1/2} = \hbar ln(2)/(\Gamma\, P_c)$ [56,86]. In this relation, Γ is the decay width of the cluster state, determined as $\Gamma = \hbar\nu P$, where ν is the assault frequency that can be defined as [83,86]

$$\nu = \frac{\hbar}{2\mu}\left[\int_{R_1}^{R_2}\frac{dR}{\sqrt{\frac{2\mu}{\hbar^2}(|V_{\rm Tot}(R)-Q|)}}\right]^{-1}. \qquad (4)$$

Also, P is the penetration probability that can be calculated by using the semiclassical WKB approximation as [61,83]

$$P = \exp\left[\frac{-2}{\hbar}\int_{R_1}^{R_2}\sqrt{2\mu(|V_{\rm Tot}(R)-Q|)}dR\right], \qquad (5)$$

where R_1 and R_2 indicates classical turning points for the cluster-daughter potential barrier that are obtained by $V_{\rm Tot}(R) = Q$. Also, P_c is the preformation probability of the cluster inside the parent nucleus.

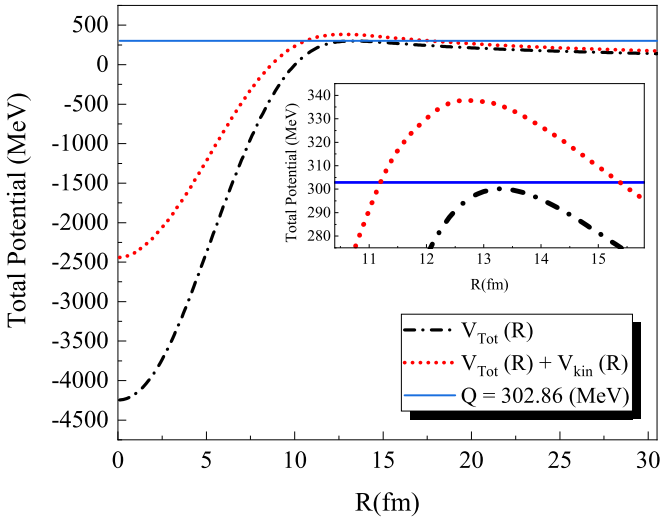

FIG. 1. The variation of the interaction potential after the PEP inclusion for the decay process of $^{294}\mathrm{Og} \rightarrow {}^{208}\mathrm{Pb} + {}^{86}\mathrm{Kr}$.

III. RESULTS AND DISCUSSION

The nucleon density distribution functions of the participating nuclei would be indispensable for a density-dependent formalism such as the DF formalism. On the other hand, a good understanding of nuclear structures has been achieved by various Skyrme forces associated with the various nuclear-matter properties [87,88]. This approach has been proven successful in describing the properties of finite nuclei. Furthermore, the HF model associated with the effective Skyrme force has been developed to account for examining the ground-state properties of nuclei. Here, determining a specified mean field that can describe the ground-state properties of the participating nuclei in the heavy-cluster radioactivity process would be beneficial to have more realistic results. Hence, in this study, the density distributions are determined by self-consistent Skyrme-HF calculations.

The HF approximation is based on a trial variational wave function, which is assumed to be an independent quasiparticle state $|\Phi\rangle$. This state, which mixes eigenstates of the particle number operator, is a linear combination of independent particle states representing various possibilities of occupying pairs of single-particle states. Furthermore, the radial part of the wave functions can be chosen to be real. Thus, the following ansatz,

$$\varphi_i(E, \mathbf{r}\sigma) = \frac{u_i(n\ell j, r)}{r} Y^{\ell}_{m_\ell}(\hat{r})\langle \ell m_\ell \frac{1}{2}\sigma | jm\rangle, \ i = 1, 2, \quad (6)$$

can be used for the wave functions. Consequently, the local densities can be written using the radial functions (omitting the isospin quantum number)

$$\rho(r) = \sum_i \varphi(E_i, r)^2 = \frac{1}{4\pi r^2} \sum_{n\ell j} (2j+1) u_2^2(n\ell j, r). \quad (7)$$

Generally, the sudden approximation is used in the DF formalism, in which the densities of the interacting nuclei are assumed to be frozen at all distances during the interaction. Therefore, one can expect that the densities of the nucleons in the compound system increase as the folding density distributions of the cluster and daughter nuclei begin at the nuclear surface and rise to full overlap. Meanwhile, the effect of PEP would be more apparent following this accumulation of nucleons. Hence, a variation in the kinetic energy at constant volume would be expected. On the other hand, the PEP is well embedded in density functional theory, manifesting as the kinetic energy term in the total Hamiltonian. This term is an obstacle to the complete overlap of the two nuclei, leading to roughly twice the normal matter, $\rho \approx 2\rho_0$, to conserve the dinuclear system around the saturation density. The mentioned kinetic energy could be determined by the extended Thomas-Fermi (ETF) approach [75,76,89]. These variations are used as a correction term into the core-cluster daughter potential obtained by the DF approach based on standard M3Y-Reid effective *NN* interaction. The kinetic-energy contribution, well-illustrated in the density functional theory, can

TABLE I. The logarithms of the various cluster-decay half-lives from ^{282}Cn within the standard M3Y and modified M3Y potentials. Note that each kind of emitted cluster refers to its most probable isotopes with the maximum Q value. The half-lives are calculated in units of seconds.

Daughter	Cluster	Q_c (MeV)	$\log_{10}(T^{(1)}_{1/2})$	$\log_{10}(T^{(2)}_{1/2})$
^{274}Hs	^{8}Be	20.38	16.39	16.61
^{268}Sg	^{14}C	38.99	18.83	21.41
^{266}Rf	^{16}O	53.47	25.44	30.64
^{254}Fm	^{28}Mg	92.93	25.91	30.15
^{250}Cf	^{32}Si	111.72	25.81	30.32
^{244}Cm	^{38}S	127.22	27.97	33.08
^{236}Pu	^{46}Ar	145.65	26.63	31.66
^{234}U	^{48}Ca	164.89	23.61	28.68
^{231}Pa	^{51}Sc	168.61	26.57	32.43
^{228}Th	^{54}Ti	177.64	24.59	30.64
^{227}Ac	^{55}V	182.10	27.25	33.22
^{224}Ra	^{58}Cr	191.82	24.01	30.26
^{221}Fr	^{61}Mn	197.27	24.69	31.36
^{216}Rn	^{66}Fe	208.63	19.99	26.24
^{213}At	^{69}Co	215.56	19.37	25.33
^{210}Po	^{72}Ni	228.99	13.34	18.67
^{209}Bi	^{73}Cu	236.06	12.35	17.39
^{208}Pb	^{74}Zn	246.32	8.13	13.36
^{205}Tl	^{77}Ga	248.62	10.25	15.54
^{202}Hg	^{80}Ge	255.69	8.41	13.44
^{201}Au	^{81}As	257.75	10.48	15.81
^{198}Pt	^{84}Se	264.66	8.19	13.45
^{197}Ir	^{85}Br	265.65	10.88	16.37
^{194}Os	^{88}Kr	270.94	9.17	15.26
^{191}Re	^{91}Rb	270.91	11.95	18.01
^{188}W	^{94}Sr	276.33	9.80	15.97
^{187}Ta	^{95}Y	276.92	11.76	18.48
^{184}Hf	^{98}Zr	281.61	9.89	16.92
^{179}Lu	^{103}Nb	282.90	10.62	17.58
^{178}Yb	^{104}Mo	288.86	7.99	14.87

TABLE II. The logarithms of the heavy-cluster-decay half-lives for even-even heavy-cluster emissions from SHN within the DF and modified DF formalisms and the comparison with the CPPM and ASAF models [44,49]. The half-lives are calculated in units of seconds. The uncounted units of $T_{1/2}^{(1)}$ indicate that the $V_{\rm Tot}(R) = Q$ cannot be established within the standard M3Y interaction.

Parent	Cluster	Q_c (MeV)	Skyrme force	$\log_{10}(T_{1/2}^{(1)})$	$\log_{10}(T_{1/2}^{(2)})$	$\log_{10}(T_{1/2}^{\rm ASAF})$ [44]	$\log_{10}(T_{1/2}^{\rm CPPM})$[49]
^{252}Fm	^{48}Ca	145.81	KDE [106]	19.79	24.63	23.63	24.89
^{278}Hs	^{72}Ni	216.92	KDE [106]	11.93	17.71	16.76	17.82
^{282}Ds	^{74}Ni	222.91	v080 [107]	11.28	16.76	15.21	16.70
^{282}Cn	^{74}Zn	244.88	v080 [107]	7.01	12.28	9.29	12.42
^{284}Cn	^{76}Zn	244.55	v080 [107]	6.70	11.93	8.91	12.02
^{284}Fl	^{78}Ge	263.38	MSk1 [108]	4.20	9.47	6.71	9.65
^{286}Fl	^{80}Ge	263.23	MSk1 [108]	3.75	9.07	6.18	9.07
^{288}Fl	^{80}Ge	263.66	MSk1 [108]	2.93	8.08	5.12	8.35
^{290}Fl	^{82}Ge	262.97	MSk1 [108]	3.05	7.90	5.30	8.20
^{294}Fl	^{82}Ge	256.92	MSk1 [108]	6.61	12.37	10.81	12.67
^{292}Lv	^{84}Se	283.65	SLy7 [88]	—	3.50	0.55	3.29
^{294}Og	^{86}Kr	302.86	SLy7 [88]	—	0.31	−2.45	0.84
^{300}120	^{92}Sr	320.82	SLy7 [88]	—	−4.23	−5.73	−6.57
^{302}120	^{94}Sr	319.65	SLy7 [88]	—	−4.16	−5.26	−6.41

be obtained by [90,91]

$$\Delta K(R) = \frac{\hbar^2}{2m}\iint\{\tau[\rho_{1p}(\mathbf{r}) + \rho_{2p}(\mathbf{r}-\mathbf{R}), \rho_{1n}(\mathbf{r}) + \rho_{2n}(\mathbf{r}-\mathbf{R})] - \tau[\rho_{1p}(\mathbf{r}) + \rho_{1n}(\mathbf{r})] - \tau[\rho_{2p}(\mathbf{r}) + \rho_{2n}(\mathbf{r})]\}d\mathbf{r}, \quad (8)$$

where τ denotes the kinetic-energy density, ρ_{ip} and ρ_{in}, $i = 1$ and 2, denote the proton and neutron density distributions at the specified interacting points of the cluster and daughter nuclei, respectively. The two nuclei are overlapping at R and completely separated at infinity, $R = \infty$. In the above equation, the first bracket denotes the kinetic-energy contribution of the dinuclear system. The second and third brackets represent the same energy for cluster and daughter nuclei at the separated configuration. The contribution of the kinetic-energy density for the dinuclear system coincides with the overlapping densities of the heavy cluster and daughter nuclei, which would be quantified by the ETF approach and considering the semiclassical correction of the second-order $\hbar$ [92]

TABLE III. The logarithms of the heavy-cluster-decay half-lives for even-odd heavy-cluster emissions from SHN within the DF and modified DF formalisms and the comparison with the ASAF and CPPM models [44,49]. The half-lives are calculated in units of seconds. The uncounted units of $T_{1/2}^{(1)}$ indicate that the $V_{\rm Tot}(R) = Q$ cannot be established within the standard M3Y interaction.

Parent	Cluster	Q_c (MeV)	Skyrme force	$\log_{10}(T_{1/2}^{(1)})$	$\log_{10}(T_{1/2}^{(2)})$	$\log_{10}(T_{1/2}^{\rm ASAF})$ [44]	$\log_{10}(T_{1/2}^{\rm CPPM})$ [49]
^{265}Rf	^{55}Ti	164.29	KDE [106]	20.05	26.15	26.71	26.32
^{267}Rf	^{61}Cr	176.21	KDE [106]	19.86	26.08	28.83	26.21
^{269}Sg	^{64}Fe	196.01	KDE [106]	17.86	23.46	24.94	23.38
^{271}Sg	^{65}Fe	195.87	KDE [106]	16.90	23.01	24.86	23.12
^{273}Hs	^{68}Ni	216.63	KDE [106]	14.21	19.50	20.25	19.30
^{275}Hs	^{70}Ni	216.71	KDE [106]	13.44	18.65	19.97	18.69
^{277}Hs	^{71}Ni	216.50	KDE [106]	12.74	18.58	19.76	18.44
^{279}Ds	^{71}Ni	224.81	v080 [107]	10.41	15.92	15.77	16.02
^{281}Ds	^{72}Ni	223.17	v080 [107]	11.20	16.70	17.05	16.91
^{281}Cn	^{74}Zn	244.77	v080 [107]	7.24	12.65	12.15	12.67
^{283}Cn	^{76}Zn	244.38	v080 [107]	7.02	12.49	12.00	12.33
^{285}Cn	^{77}Zn	243.55	v080 [107]	7.30	12.55	12.26	12.53
^{287}Fl	^{80}Ge	263.61	MSk1 [108]	3.45	8.34	8.04	8.56
^{289}Fl	^{81}Ge	263.06	MSk1 [108]	3.21	8.44	8.22	8.50
^{291}Lv	^{84}Se	283.60	SLy7[88]	−1.02	3.73	3.58	3.55
^{293}Lv	^{85}Se	282.19	SLy7 [88]	−0.96	4.21	4.34	4.22
^{295}Og	^{87}Kr	302.10	SLy7 [88]	—	0.44	0.50	−0.56
^{299}120	^{91}Sr	320.58	SLy7 [88]	—	−3.46	−2.70	−5.61
^{301}120	^{93}Sr	319.73	SLy7 [88]	—	−3.82	−3.86	−5.83

TABLE IV. The logarithms of the heavy-cluster-decay half-lives for odd-even and odd-odd heavy-cluster emissions from SHN within the DF and modified DF formalisms and the comparison with the ASAF and CPPM models [44,49]. The half-lives are calculated in units of seconds. The uncounted units of $T_{1/2}^{(1)}$ indicate that the $V_{\rm Tot}(R) = Q$ cannot be established within the standard M3Y interaction.

Parent	Cluster	Q_c (MeV)	Skyrme force	$\log_{10}\left(T_{1/2}^{(1)}\right)$	$\log_{10}\left(T_{1/2}^{(2)}\right)$	$\log_{10}\left(T_{1/2}^{\rm ASAF}\right)$ [44]	$\log_{10}\left(T_{1/2}^{\rm CPPM}\right)$ [49]
^{253}Es	^{46}Ar	129.69	Zs [87]	21.24	25.70	25.87	26.19
^{278}Bh	^{73}Ni	211.50	KDE [106]	13.81	19.83	22.73	19.81
^{282}Mt	^{71}Co	207.73	v080 [107]	16.53	22.60	25.44	22.65
^{286}Rg	^{78}Cu	230.24	v080 [107]	10.92	16.45	18.88	16.40
^{287}Nh	^{79}Ga	253.22	v080 [107]	5.69	10.82	8.97	10.65
^{290}Nh	^{81}Ga	250.41	v080 [107]	7.07	12.38	13.45	12.18
^{297}119	^{89}Rb	311.08	SLy7 [88]	—	−1.29	−1.71	−2.70
^{299}119	^{91}Rb	310.19	SLy7 [88]	—	−1.50	−1.52	−2.81
^{300}119	^{92}Rb	308.96	SLy7 [88]	—	−0.94	1.56	−1.99

proposed as

$$\tau_q(\mathbf{r}) = \frac{3}{5}(3\pi^2)^{\frac{2}{3}}\rho_q^{\frac{5}{3}} + \frac{1}{36}\frac{(\nabla\rho_q)^2}{\rho_q} + \frac{1}{3}\Delta\rho_q + \frac{1}{6}\frac{\nabla\rho_q\cdot\nabla f_q}{f_q} + \frac{1}{6}\rho_q\frac{\Delta f_q}{f_q} - \frac{1}{12}\rho_q\left(\frac{\nabla f_q}{f_q}\right)^2 + \frac{1}{2}\rho_q\left(\frac{2m}{\hbar^2}\right)^2\left(\frac{W_0}{2}\frac{\nabla(\rho+\rho_q)}{f_q}\right)^2, \tag{9}$$

where q denotes proton and neutron and $f_q(\vec{r})$ is the effective-mass form factor that is given by

$$f_q(\mathbf{r}) = 1 + \frac{2m}{\hbar^2}\frac{1}{4}\left[t_1\left(1+\frac{x_1}{2}\right) + t_2\left(1+\frac{x_2}{2}\right)\right]\rho(\mathbf{r}) - \frac{2m}{\hbar^2}\frac{1}{4}\left[t_1\left(x_1+\frac{1}{2}\right) - t_2\left(x_2+\frac{1}{2}\right)\right]\rho_q(\mathbf{r}). \tag{10}$$

The nuclear densities $\rho = \rho_1 + \rho_2$ are obtained from HF calculations based on various Skyrme forces, and m is the nucleon mass. The parameters x_1, x_2, t_1, t_2, and W_0 are obtained by fitting different properties of nuclei.

One should note that the repulsive force between the interacting nuclei due to Pauli blocking increases the internal energy of the overlapping system. Such variations in the internal energy of the dinuclear system are not embedded in the DF formalism. The energy deviation in the dinuclear system could be manifested as an increase in the kinetic energy of the nucleons. Hence, the kinetic energy estimated by the ETF approach for the dinuclear system can be considered as a corrective term in the DF model. To have a better insight into the effect of the PEP, the total interaction potential for the ^{86}Kr cluster emission from the ^{294}Og emitter is explicitly presented in Fig. 1. The results presented in Fig. 1 indicate that the influence of the considered kinetic energy on the interior regions of the Coulomb barrier is quite evident. This kinetic energy due to the PEP acts as a repulsive force that hinders a large density overlap, gradually reduces the depth of the attractive total potential in the dinuclear system, and increases the width and height of the Coulomb barrier. Thus, one can expect that the embedding of the PEP would affect the interaction potential and the subsequent half-lives.

One should note that the nucleon density distributions used for calculating interaction potentials are obtained by the Skyrme interactions selected with the best description of the binding energy and rms radii of parent, daughter, and clusters. It is noticeable that the deviation of the kinetic energy, due to the PEP, in the dinuclear system is also being calculated at the same mean field employed for each decay process.

Since the atomic masses of some SHN have not been reported yet, the WS4 + RBF mass model is employed to estimate Q values of α emission and other heavy clusters' emission [93]. One should consider that the WS4 + RBF mass model has high accuracy in estimations of the binding energies and α-decay energies for the wide extended nuclei.

In the preformed cluster models, the emitted cluster and the daughter are supposed to be preformed individually inside the parent nucleus with a definite preformation probability. Subsequently, the emitted particle tries to tunnel through the

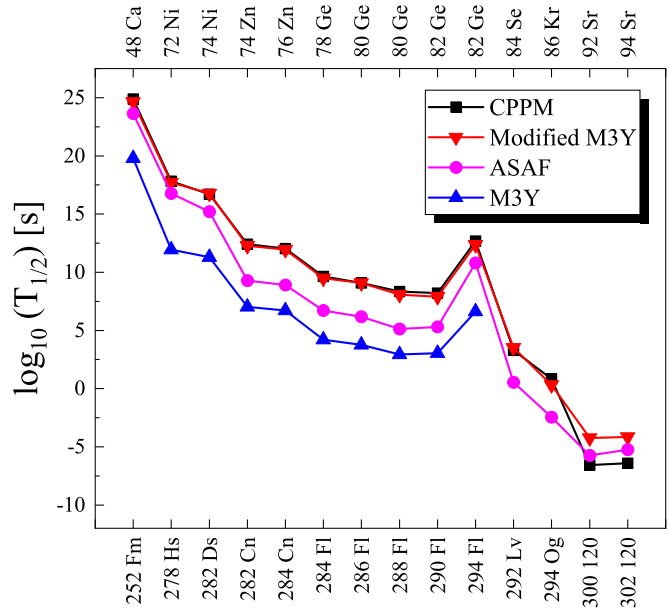

FIG. 2. The logarithms of the cluster-decay half-lives for even-even heavy-cluster emissions from SHN and the comparison with the obtained results by the ASAF and CPPM models.

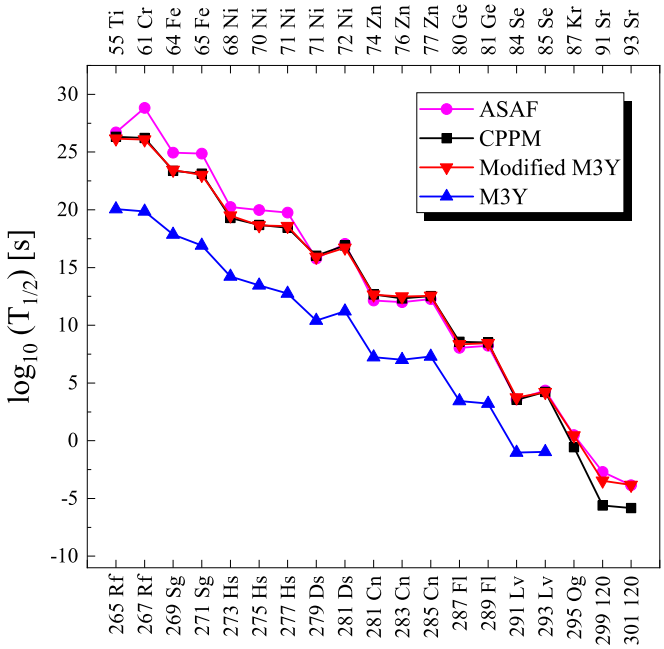

FIG. 3. The logarithms of the cluster-decay half-lives for even-odd heavy-cluster emissions from SHN and the comparison with the obtained results by the ASAF and CPPM models.

confining Coulomb barrier between the two formed clusters in the parent nucleus. Of course, the nuclear properties of the formed daughter and cluster, such as their formation energies, could strongly affect the decaying process. Therefore, a good determination of preformation probability can provide more reliable knowledge about nuclear structure, especially

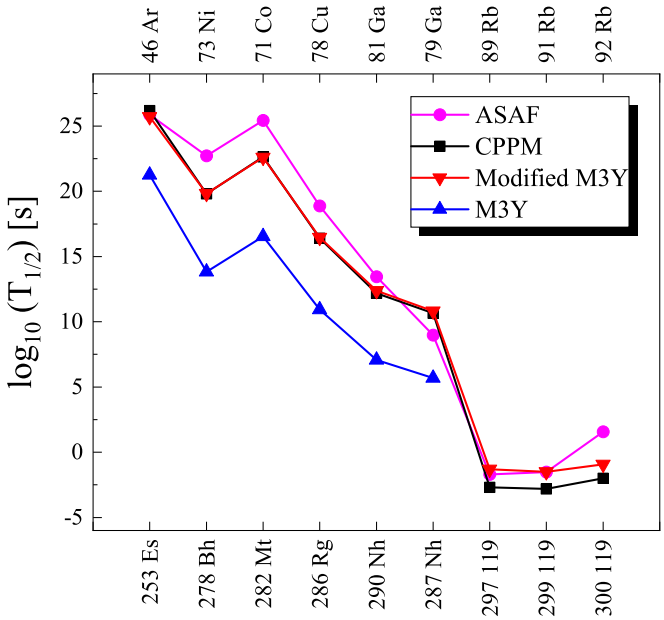

FIG. 4. The logarithms of the cluster-decay half-lives for odd-even and odd-odd heavy-cluster emissions from SHN and the comparison with the obtained results by the ASAF and CPPM models.

the dynamic states of nucleons around the nuclear surface and clusterization effects. Hence, multiple investigations have been done for such an intention. Meanwhile, it is reported that the energy-dependent preformation probability can well reproduce the α-decay and heavy-cluster-decay widths [49,94]. For instance, one can refer to the extracted Q-dependent formation probability reproducing more consistent cluster-decay half-lives with experimental data that is suggested as [49]

$$P_c = 10^{aQ^2+bQ+c}, \tag{11}$$

where the parameters a, b, and c are 6.37291×10^{-4}, -0.25736, and 3.35106, respectively. Although the present Q-dependent formation probability can well reproduce most experimental decay widths, its calculation can still be improved by more consistently calculated half-lives with experimental data that are employed for extracting an optimized fitted Q-dependent formation probability. Subsequently, considering such consistent half-lives would lead to a more accurate Q-dependent formation probability.

More importantly, in our previous work, the effects of the PEP were investigated for the observed heavy-cluster radioactivity at the superheavy region with $87 \leqslant Z \leqslant 96$. This investigation was conducted by considering the effects of additional repulsive forces due to the PEP in the density overlapping regions as an increase in the kinetic energy in the dinuclear system. The results indicated that the obtained half-lives by applying such correction terms in the DF formalism could lead to more consistent values with experimental data [95].

Consequently, the preformation probabilities introduced in Eq. (11) become refitted to the more consistent half-lives obtained in our previous work to have more precise results. One should note that such half-lives were estimated for the observed heavy-cluster radioactivities. As a result of the fit process, the parameters a', b', and c' are 5.22662×10^{-4}, -0.22272, and 3.730 06 are achieved, respectively, which is used in the following. Encouragingly, this refitted relation results in the physical preformation probabilities with the values $0 \leqslant \acute{P}_c \leqslant 1$.

Consequently, to determine the dominant cluster radioactivity in the superheavy region with $100 \leqslant Z \leqslant 120$, the half-lives of all possible heavy-cluster-decay modes even greater than $Z_{\max}$ can be calculated by employing the modified DF formalism with a kinetic-energy contribution. Consequently, the most dominant cluster-decay modes for each SHN would be determined due to the lowest obtained half-lives. Hence, a cluster with a higher Q value would be more probable in its individual isotope groups, which could be considered as one decay mode of SHN. Typically, all clusters with higher Q values than their isotope groups are considered for ^{282}Cn, as listed in Table I. One should note that all Q values of heavy-cluster radioactivities for ^{282}Cn are obtained by the WS4 + RBF mass model listed in column 3 of Table I [93]. Also, the heavy-cluster-decay half-lives of ^{282}Cn are calculated by employing the DF formalism and the modified potential with a kinetic-energy contribution within a WKB approximation listed as $T_{1/2}^{(1)}$ and $T_{1/2}^{(2)}$ in Table I. The interaction potentials are calculated within proton and neutron density

TABLE V. The α-decay and heavy-cluster-decay half-lives for even-even heavy-cluster emissions from SHN, and the corresponding branching ratios.

Parent	Q_α (MeV)	$\log_{10}\left(T^{\alpha}_{1/2}(\text{Expt.})\right)$	$\log_{10}\left(T^{\alpha}_{1/2}\right)$	Cluster	Q_c (MeV)	$\log_{10}\left(T^{c}_{1/2}\right)$	$\log_{10}$ (b)
^{274}Ds	10.892	—	−1.468	^{66}Ni	225.766	16.579	−18.047
^{276}Ds	10.868	—	−1.367	^{68}Ni	226.562	15.188	−16.555
^{278}Ds	10.226	—	0.15	^{70}Ni	225.893	15.255	−15.105
^{280}Ds	9.410	—	2.454	^{72}Ni	224.634	15.488	−13.034
^{282}Ds	8.511	—	5.463	^{74}Ni	222.909	16.764	−11.301
^{284}Ds	7.862	—	8.308	^{76}Ni	220.495	18.178	−9.869
^{286}Ds	7.745	—	8.335	^{78}Ni	218.010	19.847	−11.511
^{282}Cn	10.108	2.000	1.193	^{74}Zn	244.875	12.285	−11.091
^{284}Cn	9.514	—	2.803	^{76}Zn	244.548	11.936	−9.133
^{286}Cn	9.010	—	4.461	^{78}Zn	243.250	12.425	−7.964
^{288}Cn	9.081	—	4.17	^{80}Zn	241.562	13.460	−9.290
^{290}Cn	8.850	—	4.879	^{82}Zn	237.248	16.279	−11.400
^{286}Fl	9.936	−0.480	2.309	^{78}Ge	263.339	9.071	−6.762
^{288}Fl	9.614	−0.180	3.213	^{80}Ge	263.655	8.085	−4.872
^{290}Fl	9.491	—	3.579	^{82}Ge	262.971	7.903	−4.323
^{292}Fl	8.924	—	5.375	^{84}Ge	259.488	10.221	−4.845
^{294}Fl	8.685	—	6.279	^{86}Ge	255.184	13.203	−6.924
^{296}Fl	8.533	—	6.773	^{88}Ge	249.904	17.196	−10.423
^{290}Lv	11.052	−2.081	−0.063	^{82}Se	282.590	5.101	−5.164
^{292}Lv	11.096	−1.886	−0.243	^{84}Se	283.645	3.504	−3.747
^{294}Lv	10.635	—	0.923	^{86}Se	281.394	4.390	−3.467
^{296}Lv	10.865	—	0.327	^{88}Se	278.668	5.845	−5.518
^{298}Lv	10.743	—	0.589	^{90}Se	274.664	8.599	−8.010
^{294}Og	12.167	−3.161	−2.126	^{86}Kr	302.857	0.316	−2.442
^{296}Og	11.722	—	−1.136	^{88}Kr	301.778	0.226	−1.362
^{298}Og	12.153	—	−2.242	^{90}Kr	300.304	0.572	−2.814
^{300}Og	11.928	—	−1.765	^{92}Kr	297.665	1.889	−3.654
^{302}Og	12.014	—	−1.993	^{94}Kr	294.426	3.795	−5.788
^{304}Og	13.096	—	−4.309	^{96}Kr	292.723	4.511	−8.821
^{296}120	13.312	—	−4.003	^{88}Sr	321.274	−2.678	−1.325
^{298}120	12.977	—	−3.106	^{90}Sr	321.277	−3.548	0.442
^{300}120	13.290	—	−3.694	^{92}Sr	320.816	−4.231	0.537
^{302}120	12.862	—	−3.089	^{94}Sr	319.646	−4.159	1.071
^{304}120	12.736	—	−2.841	^{96}Sr	317.102	−2.963	0.122
^{306}120	13.761	—	−5.019	^{98}Sr	316.157	−3.135	−1.884

distributions, which are self-consistently determined by Skyrme-HF calculations with the best simultaneous descriptions of the nuclear properties of parent, daughter, and cluster nuclei. As a result, the *Zs* Skyrme interaction [87] is employed due to more consistent calculated binding energies and rms radii of the participating nuclei in the decay modes ^{282}Cn with their corresponding experimental values. The listed results in Table I express that the $^{282}\text{Cn} \rightarrow {}^{208}\text{Pb} + {}^{74}\text{Zn}$ decay process with the lowest logarithmic half-life of 13.36 s could be the dominant decay mode of ^{282}Cn. This lowest achieved half-life refers to the daughter nucleus ^{208}Pb with a double-magic closed shell, implying the strong shell effect on the heavy-cluster radioactivity. This dominant decay mode agrees with the ASAF model [40,44].

To further explore the heavy-cluster radioactivity in the superheavy region with $100 \leqslant Z \leqslant 120$, a systematic investigation would be required for a wide range of the SHN. Hence, half-lives of all possible heavy-cluster-decay modes are calculated using the modified DF formalism with a kinetic-energy contribution. Consequently, the most dominant cluster decay modes for each SHN are being determined, listed in Tables II–IV in the second column. It is worth mentioning that various successful theoretical studies have exposed the possibility of heavy-cluster emission from SHN in the $100 \leqslant Z \leqslant 120$ regions [28,40,43,44]. To achieve such intention, the heavy-cluster-decay half-lives for SHN with $100 \leqslant Z \leqslant 120$ are calculated by the DF potential and the modified DF potential, with a kinetic-energy contribution, that are respectively listed as $T^{(1)}_{1/2}$ and $T^{(2)}_{1/2}$ in Tables II–IV. It is noticeable that the calculations were carried out by considering the same and constant mean field, which simultaneously describes the ground-state properties of participating nuclei in the specific decay process. These selected mean fields are listed in Tables II–IV.

For comparison, the mentioned obtained heavy-cluster-decay half-lives can be evaluated with their corresponding values that are other theoretical models. As shown in Refs. [44,49,96,97], the ASAF and CPPM models reproduced

TABLE VI. The α-decay and heavy-cluster-decay half-lives for even-odd heavy-cluster emissions from SHN, and the corresponding branching ratios.

Parent	Q_α (MeV)	$\log_{10}\left(T^{\alpha}_{1/2}(\text{Expt.})\right)$	$\log_{10}\left(T^{\alpha}_{1/2}\right)$	Cluster	Q_c (MeV)	$\log_{10}\left(T^{c}_{1/2}\right)$	$\log_{10}$ (b)
^{279}Ds	9.834	−0.678	1.318	^{71}Ni	224.814	15.924	−14.606
^{281}Ds	8.956	2.140	3.933	^{73}Ni	223.404	16.273	−12.340
^{283}Ds	8.142	—	6.963	^{75}Ni	221.424	17.581	−10.617
^{285}Ds	7.781	—	8.303	^{77}Ni	219.078	19.223	−10.921
^{285}Cn	9.203	1.447	3.915	^{77}Zn	243.548	12.556	−8.641
^{287}Cn	9.036	—	4.463	^{79}Zn	242.147	13.144	−8.681
^{289}Cn	9.021	—	4.552	^{81}Zn	239.146	15.032	−10.479
^{291}Fl	9.241	—	4.446	^{83}Ge	261.074	9.110	−4.663
^{295}Fl	8.579	–	6.732	^{87}Ge	252.092	15.641	−8.909
^{293}Lv	10.763	−1.244	0.767	^{85}Se	282.194	4.212	−3.445
^{295}Lv	10.744	—	0.774	^{87}Se	279.642	5.542	−4.768
^{297}Lv	10.807	—	0.640	^{89}Se	276.303	7.639	−6.999
^{295}Og	11.872	—	−1.384	^{87}Kr	302.099	0.446	−1.830
^{297}Og	12.074	—	−1.876	^{89}Kr	300.635	0.983	−2.859
^{299}Og	12.017	—	−1.836	^{91}Kr	298.540	1.662	−3.498
^{297}120	13.113	—	−3.389	^{89}Sr	321.105	−2.902	−0.488
^{301}120	13.036	—	−3.377	^{93}Sr	319.729	−3.821	0.443
^{303}120	12.783	—	−2.932	^{95}Sr	318.098	−3.414	0.482

well the α-decay and cluster-decay half-lives of SHN. Hence, these models are adopted to further compare heavy-cluster radioactivity predictions in the superheavy region. Therefore, the logarithms of the cluster-decay half-lives obtained by ASAF and CPPM models are presented as $T^{\text{ASAF}}_{1/2}$ and $T^{\text{CPPM}}_{1/2}$ in Tables II–IV, respectively. The comparison of the obtained half-lives within the ASAF and CPPM models and those obtained by M3Y and modified M3Y potentials confirms that the calculated half-lives within simultaneous kinetic-energy modification and cluster preformation factor applications obtained by our refitted relation can lead to more consistent half-lives with other theoretical investigations. In order to have a visual perception, the half-lives obtained by the standard M3Y and modified M3Y potentials and their corresponding values obtained by ASAF and CPPM models classified in terms of the parent nuclei and cluster emissions are shown in Figs 2–4. The presented results in these figures express a remarkable improvement in the consistency of the heavy-cluster-decay half-lives obtained by the DF potential modified by considering the kinetic-energy contribution and those obtained by ASAF and CPPM models. Therefore, considering the repulsive kinetic-energy correction term to the DF

TABLE VII. The α-decay and heavy-cluster-decay half-lives for odd-even heavy-cluster emissions from SHN, and the corresponding branching ratios.

Parent	Q_α (MeV)	$\log_{10}\left(T^{\alpha}_{1/2}(\text{Expt.})\right)$	$\log_{10}\left(T^{\alpha}_{1/2}\right)$	Cluster	Q_c (MeV)	$\log_{10}\left(T^{c}_{1/2}\right)$	$\log_{10}$ (b)
^{282}Rg	9.300	2.000	3.304	^{74}Cu	233.677	15.008	−11.704
^{284}Rg	8.660	—	5.393	^{76}Cu	232.294	15.215	−9.821
^{286}Rg	8.415	—	6.279	^{78}Cu	230.240	16.459	−10.180
^{288}Rg	8.405	—	6.272	^{80}Cu	226.923	18.667	−12.395
^{286}Nh	9.460	0.978	3.463	^{78}Ga	253.288	11.175	−7.712
^{288}Nh	9.317	—	3.940	^{80}Ga	252.420	11.267	−7.327
^{290}Nh	9.132	—	4.554	^{82}Ga	250.069	12.513	−7.958
^{288}Mc	10.363	−0.785	1.553	^{80}As	271.927	8.105	−6.552
^{292}Mc	9.902	—	2.770	^{84}As	271.325	7.232	−4.461
^{294}Mc	9.668	—	3.429	^{86}As	268.083	9.129	−5.699
^{296}Mc	9.579	—	3.735	^{88}As	263.985	12.081	−8.345
^{294}Ts	11.346	−1.292	−0.393	^{86}Br	291.744	2.753	−3.145
^{296}Ts	11.473	—	−0.753	^{88}Br	289.937	3.453	−4.205
^{298}Ts	11.490	−0.180	−0.835	^{90}Br	287.164	4.859	−5.694
^{300}Ts	11.521	—	−0.946	^{92}Br	283.855	6.834	−7.780
^{298}119	12.684	—	−2.880	^{90}Rb	310.410	−1.079	−1.801
^{300}119	12.543	—	−2.588	^{92}Rb	308.963	−0.938	−1.650
^{302}119	12.398	—	−2.357	^{94}Rb	306.661	0.446	−2.803
^{304}119	12.902	—	−3.470	^{96}Rb	304.176	1.398	−4.868

TABLE VIII. The α-decay and heavy-cluster-decay half-lives for odd-odd heavy-cluster emissions from SHN, and the corresponding branching ratios.

Parent	Q_α (MeV)	$\log_{10}\left(T^{\alpha}_{1/2}(\text{Expt.})\right)$	$\log_{10}\left(T^{\alpha}_{1/2}\right)$	Cluster	Q_c (MeV)	$\log_{10}\left(T^{c}_{1/2}\right)$	$\log_{10}$ (b)
^{283}Rg	8.998	—	4.154	^{75}Cu	233.416	14.513	−10.359
^{285}Rg	8.431	—	6.136	^{77}Cu	231.621	15.487	−9.351
^{287}Rg	8.415	—	6.176	^{79}Cu	229.607	16.816	−10.640
^{283}Nh	10.372	−1.125	−0.074	^{75}Ga	253.410	11.984	−12.058
^{285}Nh	9.778	0.623	2.411	^{77}Ga	253.692	11.115	−8.705
^{287}Nh	9.315	—	3.858	^{79}Ga	253.215	10.825	−6.966
^{289}Nh	9.292	—	3.941	^{81}Ga	252.029	11.266	−7.324
^{291}Nh	8.880	—	5.228	^{83}Ga	248.075	13.814	−8.585
^{287}Mc	10.467	−1.432	1.268	^{79}As	271.643	8.723	−7.454
^{289}Mc	10.263	−0.481	1.742	^{81}As	272.794	7.156	−5.413
^{291}Mc	10.162	—	1.921	^{83}As	272.931	6.267	−4.346
^{293}Mc	9.684	—	3.317	^{85}As	270.046	7.911	−4.594
^{295}Mc	9.695	—	3.298	^{87}As	266.570	10.036	−6.738
^{297}Mc	9.564	—	3.654	^{89}As	261.857	13.492	−9.837
^{293}Ts	11.591	−1.658	−1.074	^{85}Br	292.841	2.262	−3.336
^{295}Ts	11.266	—	−0.323	^{87}Br	291.182	2.895	−3.218
^{297}Ts	11.589	—	−1.167	^{89}Br	289.153	3.468	−4.635
^{299}Ts	11.430	—	−0.765	^{91}Br	285.884	5.544	−6.309
^{301}Ts	11.584	—	−1.126	^{93}Br	282.298	7.770	−8.896
^{297}119	12.394	—	−2.356	^{89}Rb	311.079	−1.299	−1.057
^{299}119	12.735	—	−3.161	^{91}Rb	310.194	−1.505	−1.656
^{301}119	12.398	—	−2.475	^{93}Rb	308.297	−0.750	−1.724
^{303}119	12.389	—	−2.338	^{95}Rb	305.374	0.894	−3.233
^{305}119	13.398	—	−4.546	^{97}Rb	303.888	1.074	−5.621

formalism can productively promote the prediction of heavy-cluster radioactivities and adequately describe their properties in the superheavy region.

Furthermore, it has been shown that the α-decay half-lives in the heavy- and superheavy-mass regions with $82 \leqslant Z \leqslant 120$, calculated by identical modification of the DF formalism and applying the cluster preformation probability estimated by the cluster formation model (CFM) can lead to a better reproduction of the experimental α-decay widths [98].

Eventually, according to such better compatibility of the modified DF formalism in interaction potential calculations for α and other heavy-cluster cases, determining the competition between α and other heavy clusters would be desirable. To this end, even-even, even-odd, and odd-odd SHN with $110 \leqslant Z \leqslant 120$ were selected, leading to the double-magic closed-shell ^{208}Pb with their heavy-cluster-decay modes. The reason is that such decaying systems have a strong clusterlike structure ($A = {}^{208}\text{Pb} \bigotimes c$) in which the parent nuclei decay only once, like α decay. It should be noted that for calculating the α-core interaction potential, the Gaussian density distribution function is used for α particles in this study [99].

Consequently, the α-decay and heavy-cluster-decay half-lives of wide-extended SHN are calculated by modified M3Y potentials listed as $T^{\alpha}_{1/2}$ and $T^{c}_{1/2}$ in Tables V–VIII. Also, the experimental α-decay half-lives of the known SHN are presented as $T^{\alpha}_{1/2}$(Expt.) in Tables V–VIII [100,101]. It should be noted that the α-formation probability has a remarkable role in the α-decay studies [65,102,103]. In this investigation, due to the energy dependence of the cluster preformation probabilities introduced in Eq. (11), the energy-dependent α-preformation probabilities would be required. On the other hand, the CFM represents the intended energy-dependent α-preformation probabilities in terms of cluster formation and total energies. Furthermore, such preformation probabilities obtained by CFM are consistent with the corresponding values reported by Varga *et al.* [104,105]. It should be noted that the cluster-decay half-lives of all these isotopes listed in TablesV–VIII are in a measurable range of less than 10^{30} s [97], implying that heavy-cluster radioactivities can occur for the mentioned isotopes. Also, one should consider that there are no experimental data on heavy-cluster emission of SHN with $110 \leqslant Z \leqslant 120$ presently.

According to the calculated α-decay and heavy-cluster-decay half-lives listed in Tables V–VIII, to clarify the intended competition between α decay and heavy-cluster radioactivity, the evaluation of the branching ratio between cluster radioactivity and their corresponding α decay would be beneficial, which is calculated as

$$b = \frac{\lambda_c}{\lambda_\alpha} = \frac{T_\alpha}{T_c}, \tag{12}$$

where λ_c and T_c are the decay constant and the half-life for cluster radioactivity and λ_α and T_α are the decay constant and the half-life for α emission.

According to the presented results in Tables V–VIII, several isotopes would have heavy-cluster radioactivities that are more preferred than the α-decay mode. Consequently, the logarithmic branching ratios for isotopes of elements $Z = 120$ and $A = 298$ and 300–304 with heavy clusters ($^{90,92-96}$Sr) are obtained as 0.442, 0.537, 0.443, 1.071, 0.482, and 0.122

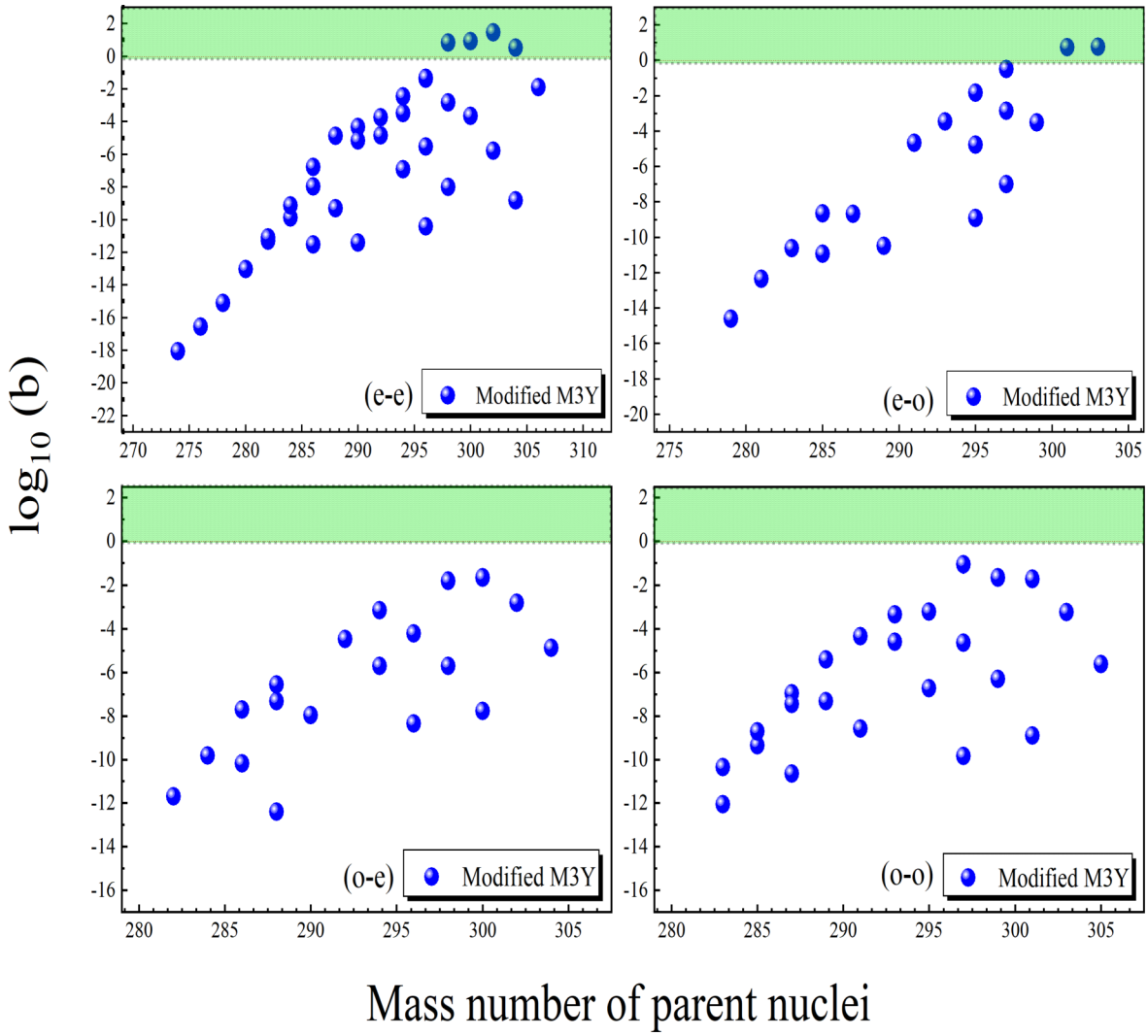

FIG. 5. The branching ratio of the calculated half-lives within modified M3Y interaction for even-even, even-odd, odd-even, and odd-odd heavy-cluster emissions and α decay in terms of the mass number of the parent nuclei. The colored region indicates the branching ratio of the probable heavy-cluster radioactivity.

respectively. In addition, to have a better insight into these results, the logarithmic values of branching ratios for the most probable emitted clusters in terms of the mass number of parent nuclei originated through the modified DF formalism are presented in Fig. 5.

As shown in Fig. 5, one can see that the isotopes of $^{298,300-304}120$ have positive branching ratios expressing higher probabilities of heavy cluster radioactivities than α decay. On the other hand, one should note that the branching ratios reported by the CPPM model for the same isotopes $^{298,300-304}120$ are 0.338, 0.506, 0.199, 1.077, -0.151, and -0.694, respectively [49]. Furthermore, it was reported by the ASAF model that $^{300,302}120$ are the possible cluster emitters with branching ratios of -0.10 and 0.49, respectively [44]. Hence, these isotopes could be supposed to be the heavy-cluster emitters. These results reveal that the branching ratio using the modified DF formalism and CPPM and ASAF models reasonably agree. Also, the study suggests that the modified DF formalism can effectively predict the heavy-cluster emission from the superheavy regions.

IV. SUMMARY AND CONCLUSION

This study investigates the probable heavy-cluster radioactivity of superheavy isotopes with $100 \leqslant Z \leqslant 120$ within the modified DF formalism by the PEP inclusion. The PEP is investigated by considering an increase in the kinetic energy in the dinuclear systems. To this intention, the ETF approach estimates such kinetic energies that have arisen in overlapping regions. Subsequently, the results showed that some energy variations in the internal region of the interaction potentials would be expected, affecting the heavy-cluster-decay half-life calculations.

Furthermore, the cluster-decay half-lives of SHN are studied using the standard M3Y potentials and modified M3Y potentials by the PEP inclusion by increasing kinetic-energy

consideration at overlapping regions. The results indicated that the cluster-decay half-lives within modified interaction potentials associated with the PEP lead to more consistency with the predictions of other theoretical models. Also, further investigation on the competition between α decay and heavy-cluster radioactivity leading to ^{208}Pb was performed. The obtained results exposed that heavy-cluster radioactivities are more probable than α decay for some of the isotopes of $Z = 120$. The $^{298,300-304}120$ isotopes are estimated as the most probable candidates for heavy-cluster emitters. This study revealed that the present model can effectively examine the heavy-cluster radioactivity at the superheavy region.

[1] Y. T. Oganessian, J. Phys. G: Nucl. Part. Phys. **34**, R165 (2007).
[2] K. Morita, K. Morimoto, D. Kaji *et al.*, J. Phys. Soc. Jpn. **73**, 2593 (2004).
[3] S. Hofmann and G. Munzenberg, Rev. Mod. Phys. **72**, 733 (2000).
[4] J. H. Hamilton, S. Hofmann, and Y. T. Oganessian, Annu. Rev. Nucl. Part. Sci. **63**, 383 (2013).
[5] Y. T. Oganessian, Radiochim. Acta **99**, 429 (2011).
[6] Ch. E. Düllmann, M. Schädel, A. Yakushev, A. Türler, K. Eberhardt, J. V. Kratz, D. Ackermann, L. L. Andersson, M. Block, W. Brüchle, J. Dvorak, H. G. Essel, P. A. Ellison, J. Even, J. M. Gates, A. Gorshkov, R. Graeger, K. E. Gregorich, W. Hartmann, R. D. Herzberg *et al.*, Phys. Rev. Lett. **104**, 252701 (2010).
[7] S. Hofmann, Rep. Prog. Phys. **61**, 639 (1998).
[8] Y. T. Oganessian, V. K. Utyonkov, Y. V. Lobanov, F. S. Abdullin, A. N. Polyakov, I. V. Shirokovsky, Y. S. Tsyganov, G. G. Gulbekian, S. L. Bogomolov, B. N. Gikal, A. N. Mezentsev, S. Iliev, V. G. Subbotin, A. M. Sukhov, O. V. Ivanov, G. V. Buklanov, K. Subotic, M. G. Itkis, K. J. Moody, J. F. Wild *et al.*, Phys. Rev. C **62**, 041604(R) (2000).
[9] J. Khuyagbaatar *et al.*, Phys. Rev. Lett. **112**, 172501 (2014).
[10] S. Hofmann *et al.*, Eur. Phys. J. A **14**, 147 (2002).
[11] I. Muntian, S. Hofmann, Z. Patyk, and A. Sobiczewski, Acta Phys. Pol. B **34**, 2073 (2003).
[12] Yu. Ts. Oganessian, F. Sh. Abdullin, S. N. Dmitriev *et al.*, Phys. Rev. Lett. **108**, 022502 (2012).
[13] P. Mohr, Z. Fülöp, G. Gyürky, G. G. Kiss, and T. Szücs, Phys. Rev. Lett. **124**, 252701 (2020).
[14] Yu. Ts. Oganessian, V. K. Utyonkov, Yu. V. Lobanov, F. Sh. Abdullin, A. N. Polyakov, R. N. Sagaidak, I. V. Shirokovsky, Yu. S. Tsyganov, A. A. Voinov, A. N. Mezentsev *et al.*, Phys. Rev. C **79**, 024603 (2009).
[15] G. L. Zhang, X. Y. Le, and H. Q. Zhang, Phys. Rev. C **80**, 064325 (2009).
[16] X. J. Bao, Y. Gao, J. Q. Li, and H. F. Zhang, Phys. Rev. C **91**, 011603(R) (2015).
[17] X. J. Bao, S. Q. Guo, H. F. Zhang, Y. Z. Xing, J. M. Dong, and J. Q. Li, J. Phys. G: Nucl. Part. Phys. **42**, 085101 (2015).
[18] J. P. Cui, Y. L. Zhang, S. Zhang, and Y. Z. Wang, Phys. Rev. C **97**, 014316 (2018).
[19] G. Royer, J. Phys. G: Nucl. Part. Phys. **26**, 1149 (2000).
[20] Y. Wang, Z. Li, G. Yu, and Z. Hou, J. Phys. G: Nucl. Part. Phys. **41**, 079501 (2014).
[21] V. Yu. Denisov and A. A. Khudenko, Phys. Rev. C **82**, 059902(E) (2010).
[22] P. Mohr, Eur. Phys. J. A **31**, 23 (2007).
[23] D. S. Delion and A. Sandulescu, J. Phys. G: Nucl. Part. Phys. **28**, 617 (2002).
[24] Y. Z. Wang, J. Z. Gu, J. M. Dong, and B. B. Peng, Int. J. Mod. Phys. E **19**, 1961 (2010).
[25] Y. Z. Wang, Q. F. Gu, J. M. Dong, and B. B. Peng, Int. J. Mod. Phys. E **20**, 127 (2011).
[26] Y. L. Zhang and Y. Z. Wang, Nucl. Phys. A **966**, 102 (2017).
[27] J. P. Cui, Y. L. Zhang, S. Zhang, and Y. Z. Wang, Int. J. Mod. Phys. E **25**, 1650056 (2016).
[28] Y. L. Zhang and Y. Z. Wang, Phys. Rev. C **97**, 014318 (2018).
[29] R. Bonetti and A. Guglielmetti, Rom. Rep. Phys. **59**, 301 (2007).
[30] R. Bonetti, C. Chiesa, A. Guglielmetti, C. Migliorino, A. Cesana, and M. Terrani, Nucl. Phys. A **556**, 115 (1993).
[31] A. A. Ogloblin, R. Bonetti, V. A. Denisov, A. Guglielmetti, M. G. Itkis, C. Mazzocchi, V. L. Mikheev, Yu. T. Oganessian, G. A. Pik-Pichak, G. Poli, S. M. Pirozhkov, V. M. Semochkin, V. A. Shigin, I. K. Shvetsov, and S. P. Tretyakova, Phys. Rev. C **61**, 034301 (2000).
[32] A. Sandulescu, D. N. Poenaru, and W. Greiner, Sov. J. Part. Nucl. **11**, 528 (1980).
[33] H. J. Rose and G. A. Jones, Nature (London) **307**, 245 (1984).
[34] D. V. Aleksandrov, A. F. Belyatskii, Yu. A. Glukhov, E. Yu. Nikolskii, B. G. Novatskii, A. A. Ogloblin, and D. N. Stepnov, JETP Lett. **40**, 909 (1984).
[35] A. Guglielmetti, D. Faccio, R. Bonetti, S. V. Shishkin, S. P. Tretyakova, S. V. Dmitriev, A. A. Ogloblin, G. A. Pik-Pichak, N. P. van der Meulen, G. F. Steyn *et al.*, J. Phys.: Conf. Ser. **111**, 012050 (2008).
[36] S. Wang, P. B. Price, S. W. Barwick, K. J. Moody, and E. K. Hulet, Phys. Rev. C **36**, 2717 (1987).
[37] K. J. Moody, E. K. Hulet, S. Wang, and P. B. Price, Phys. Rev. C **39**, 2445 (1989).
[38] M. Hussonnois, J. F. Le Du, L. Brillard, J. Dalmasso, and G. Ardisson, Phys. Rev. C **43**, 2599 (1991).
[39] K. P. Santhosh, R. K. Biju, and A. Joseph, J. Phys. G: Nucl. Part. Phys. **35**, 085102 (2008).
[40] D. N. Poenaru, R. A. Gherghescu, and W. Greiner, Phys. Rev. Lett. **107**, 062503 (2011).
[41] N. Ashok and A. Joseph, Nucl. Phys. A **977**, 101 (2018).
[42] A. Bhagwat and R. J. Liotta, Phys. Rev. C **96**, 031302(R) (2017).
[43] D. N. Poenaru, R. A. Gherghescu, and W. Greiner, Phys. Rev. C **85**, 034615 (2012).
[44] D. N. Poenaru, H. Stöcker, and R. A. Gherghescu, Eur. Phys. J. A **54**, 14 (2018).
[45] D. Ni, Z. Ren, T. Dong, and C. Xu, Phys. Rev. C **78**, 044310 (2008).
[46] D. N. Poenaru, R. A. Gherghescu, and W. Greiner, Phys. Rev. C **83**, 014601 (2011).
[47] M. Horoi, J. Phys. G: Nucl. Part. Phys. **30**, 945 (2004).

[48] C. Qi, F. R. Xu, R. J. Liotta, and R. Wyss, Phys. Rev. Lett. **103**, 072501 (2009).
[49] K. P. Santhosh and C. Nithya, Phys. Rev. C **97**, 064616 (2018).
[50] G. Royer, Q. Ferrier, and M. Pineau, Nucl. Phys. A **1021**, 122427 (2022).
[51] N. Sowmya, H. Manjunatha, and P. Damodara Gupta, Phys. Part. Nucl. Lett. **18**, 177 (2021).
[52] N. Sowmya, H. Manjunatha, and P. Damodara Gupta, and N. Dhananjaya, Braz. J. Phys. **51**, 99 (2021).
[53] K. P. Santhosh and T. A. Jose, Phys. Rev. C **99**, 064604 (2019).
[54] X. J. Bao, H. F. Zhang, B. S. Hu, G. Royer, and J. Q. Li, J. Phys. G: Nucl. Part. Phys. **39**, 095103 (2012).
[55] Y. Qian, Z. Ren, and D. Ni, Phys. Rev. C **94**, 024315 (2016).
[56] M. Ismail, W. M. Seif, and A. Abdurrahman, Phys. Rev. C **94**, 024316 (2016).
[57] D. Ni and Z. Ren, Phys. Rev. C **82**, 024311 (2010).
[58] C. Xu and Z. Ren, Phys. Rev. C **74**, 014304 (2006).
[59] A. Adel and T. Alharbi, Nucl. Phys. A **975**, 1 (2018).
[60] W. M. Seif and A. Adel, Phys. Rev. C **99**, 044311 (2019).
[61] C. Xu and Z. Ren, Nucl. Phys. A **753**, 174 (2005).
[62] S. S. Malik and R. K. Gupta, Phys. Rev. C **39**, 1992 (1989).
[63] B. Buck and A. C. Merchant, Phys. Rev. C **39**, 2097 (1989).
[64] S. N. Kuklin, G. G. Adamian, and N. V. Antonenko, Phys. Rev. C **71**, 014301 (2005).
[65] H. F. Zhang, J. M. Dong, G. Royer, W. Zuo, and J. Q. Li, Phys. Rev. C **80**, 037307 (2009).
[66] S. K. Arun, R. K. Gupta, B. B. Singh, S. Kanwar, and M. K. Sharma, Phys. Rev. C **79**, 064616 (2009).
[67] F. R. Xu and J. C. Pei, Phys. Lett. B **642**, 322 (2006).
[68] M. Ismail and M. Seif, Int. J. Mod. Phys. E **22**, 1350010 (2013).
[69] M. Dasgupta, D. J. Hinde, J. O. Newton, and K. Hagino, Prog. Theor. Phys. Suppl. **154**, 209 (2004).
[70] I. Angeli and K. Marinova, At. Data Nucl. Data Tables **99**, 69 (2013).
[71] Z. Ren, C. Xu, and Z. Wang, Phys. Rev. C **70**, 034304 (2004).
[72] G. Satchler and W. Love, Phys. Rep. **55**, 183 (1979).
[73] A. M. Kobos, B. A. Brown, R. Lindsay, and G. R. Satchler, Nucl. Phys. A **425**, 205 (1984).
[74] A. Mukherjee, D. J. Hinde, M. Dasgupta, K. Hagino, J. O. Newton, and R. D. Butt, Phys. Rev. C **75**, 044608 (2007).
[75] V. B. Soubbotin, W. von Oertzen, X. Vinas, K. A. Gridnev, and H. G. Bohlen, Phys. Rev. C **64**, 014601 (2001).
[76] W. Seif, A. Abdelhady, and A. Adel, J. Phys. G: Nucl. Part. Phys. **45**, 115101 (2018).
[77] Ş. Mişicu and H. Esbensen, Phys. Rev. Lett. **96**, 112701 (2006).
[78] W. M. Seif, Nucl. Phys. A **878**, 14 (2012).
[79] B. Buck, J. C. Johnston, A. C. Merchant, and S. M. Perez, Phys. Rev. C **53**, 2841 (1996).
[80] A. Adel and T. Alharbi, Phys. Rev. C **92**, 014619 (2015).
[81] R. E. Langer, Phys. Rev. **51**, 669 (1937).
[82] J. J. Morehead, J. Math. Phys. **36**, 5431 (1995).
[83] N. G. Kelkar and H. M. Castaneda, Phys. Rev. C **76**, 064605 (2007).
[84] Dao T. Khoa, Phys. Rev. C **63**, 034007 (2001).
[85] S. Cwiok, W. Nazarewicz, and P. H. Heenen, Phys. Rev. Lett. **83**, 1108 (1999).
[86] W. M. Seif, M. Ismail, A. I. Refaie, and L. H. Amer, J. Phys. G: Nucl. Part. Phys. **43**, 075101 (2016).
[87] J. Friedrich and P.-G. Reinhard, Phys. Rev. C **33**, 335 (1986).
[88] E. Chabanat, P. Bonche, P. Haensel, J. Meyer, and R. Schaeffer, Nucl. Phys. A **635**, 231 (1998).
[89] M. Moghaddari Amiri and O. N. Ghodsi, Phys. Rev. C **102**, 054602 (2020).
[90] D. Vautherin and D. M. Brink, Phys. Rev. C **5**, 626 (1972).
[91] F. L. Stancu and D. M. Brink, Nucl. Phys. A **270**, 236 (1976).
[92] R. C. Black and I. I. Satija, Phys. Rev. Lett. **65**, 1 (1990).
[93] N. Wang, M. Liu, X. Z. Wu, and J. Meng, Phys. Lett. B **734**, 215 (2014).
[94] S. M. Saleh Ahmed, R. Yahaya, S. Radiman, and M. S. Yasir, J. Phys. G **40**, 065105 (2013).
[95] M. Morshedloo, O. N. Ghodsi, and M. M. Amiri, Phys. Rev. C **107**, 034610 (2023).
[96] D. N. Poenaru and W. Greiner, in *Clusters in Nuclei*, edited by C. Beck, Lecture Notes in Physics 1 (Springer, Berlin, 2010), Vol. 818, p. 1.
[97] K. P. Santhosh and B. Priyanka, Int. J. Mod. Phys. E **23**, 1450059 (2014).
[98] O. N. Ghodsi and M. M. Amiri, Phys. Rev. C **104**, 044618 (2021).
[99] D. N. Basu, J. Phys. G: Nucl. Part. Phys. **29**, 2079 (2003).
[100] J. M. Wang, H. F. Zhang, and J. Q. Li, J. Phys. G: Nucl. Part. Phys. **41**, 075109 (2014).
[101] Y. T. Oganessian and V. K. Utyonkov, Nucl. Phys. A **944**, 62 (2015).
[102] M. Ismail and A. Adel, Phys. Rev. C **86**, 014616 (2012).
[103] W. M. Seif, M. Ismail, and E. T. Zeini, J. Phys. G: Nucl. Part. Phys. **44**, 055102 (2017).
[104] K. Varga, R. G. Lovas, and R. J. Liotta, Phys. Rev. Lett. **69**, 37 (1992).
[105] K. Varga, R. G. Lovas, and R. Liotta, Nucl. Phys. A **550**, 421 (1992).
[106] B. K. Agrawal, S. Shlomo, and V. K. Au, Phys. Rev. C **72**, 014310 (2005).
[107] J. M. Pearson and S. Goriely, Phys. Rev. C **64**, 027301 (2001).
[108] F. Tondeur, S. Goriely, J. M. Pearson, and M. Onsi, Phys. Rev. C **62**, 024308 (2000).